Biol Cybern (2010) 102:95–107
DOI 10.1007/s00422-009-0359-9

ORIGINAL PAPER

Biological Cybernetics

Independence of the unimodal tuning of firing rate from theta phase precession in hippocampal place cells

Zhihua Wu · Yoko Yamaguchi

Received: 17 June 2009 / Accepted: 10 December 2009 / Published online: 30 December 2009

Abstract There are two prominent features for place cells in rat hippocampus. The firing rate remarkably increases when rat enters the cell's place field and reaches a maximum around the center of place field, and it decreases when the animal approaches the end of the place field. Simultaneously the spikes gradually and monotonically advance to earlier phase relative to hippocampal theta rhythm as the rat traverses along the cell's place field, known as temporal coding. In this paper, we investigate whether two main characteristics of place cell firing are independent or not by mainly focusing on the generation mechanism of the unimodal tuning of firing rate by using a reduced CA1 two-compartment neuron model. Based on recent evidences, we hypothesize that the coupling of dendritic with the somatic compartment is not constant but dynamically regulated as the animal moves further along the place field, in contrast to previous two-compartment modeling. Simulations show that the regulable coupling is critically responsible for the generation of unimodal firing rate profile in place cells, independent of phase precession. Predictions of our model accord well with recent observations like occurrence of phase precession with very low as well as high firing rate (Huxter et al. Nature 425:828–832, 2003) and persistency of phase precession after transient silence of hippocampus activity (Zugaro et al. Nat Neurosci 8:67–71, 2005).

Z. Wu (✉)
State Key Laboratory of Brain and Cognitive Science,
Institute of Biophysics, Chinese Academy of Sciences,
15 Datun Road, Chaoyang District, Beijing 100101, China
e-mail: wuzh@moon.ibp.ac.cn

Y. Yamaguchi
Laboratory for Dynamics of Emergent Intelligence, RIKEN Brain Science Institute, 2-1 Hirosawa, Wako-shi, Saitama 351-0198, Japan

Keywords Unimodal profile of firing rate tuning · Place cell · Dynamical coupling · Two-compartment model · Theta phase precession

1 Introduction

In rat hippocampus, place cells signal spatial respects of the animal's environment or behavior by both firing rate and temporal code (O'Keefe and Recce 1993; Skaggs et al. 1996). A place cell's firing rate significantly increases first and then decreases showing a unimodal tuning versus position when animal passes through its place field, while the timing of spikes advances monotonically to earlier phases of cycles of the ongoing field theta rhythm. Are two codes independent or coupled each other? It is an essential question related to neural encoding and neural computation.

In contrast to a large amount of studies on theta phase precession generation (see Zugaro et al. 2005 for review), mechanisms about how firing rate tuning occurs seem to attract relatively little attention. Except a few models (Lengyel et al. 2003; O'Keefe and Recce 1993), most of studies simply assume a unimodal or ramp excitatory input to account for the unimodal profile of firing rate (Harris et al. 2002; Kamondi et al. 1998; Magee 2001; Mehta et al. 2002). If such a unimodal excitatory input exists for any place cell whenever its place field is crossed, it should be affected by specific behaviors or stimuli, at least to an observable extent. However, evidences do not show a consistency. For instance, it is well documented that firing rate increases with running speed (Ekstrom et al. 2001; McNaughton et al. 1983). But the unimodal profile of firing rate seems to have no significant correlation with running speed: it putatively exists regardless of whether the highest running speed appears in the center of a place field or not. Moreover, the shape of a place field

shows a big stability in face of instant changes in parameters such as the track shape, the location of the place fields on the tracks, the behavior of the rat through the place fields, or a change in the rat's behavior with time (Mehta et al. 2000). These evidences indicate that firing rate tuning curve in CA1 pyramidal cells may not be induced by a unimodal afferent excitation alone. Instead, it may be the place cells' intrinsic properties that appear to primarily determine the occurrence of the unimodal profile of firing rate. It should be noted that another model proposes a similar input with a unimodal profile to place cells but it essentially differs from above. The model supposes that the input constraining a place cell to fire within the firing field is spatially modulated by receiving projections from a set of boundary vector cells (Burgess et al. 2000; Hartley et al. 2000). Each boundary vector cell is predicted to response maximally when the boundary of the animal's environment is at a particular distance and allocentric angle. Thus the rate profile of a place cell strongly depends on the rat's location relative to environmental boundary. The existence of boundary vector cells predicted by the model is verified recently in several areas including the subiculum (Lever et al. 2009) and medial entorhinal cortex (Solstad et al. 2008). While the model provides a possible solution to the firing profile being independent of firing phase, it depends on the extrahippocampal input. In this paper, we argue for a mechanism solely based on the intrinsic properties of place cells themselves.

Interference model is one of a few models accounting for the unimodal tuning of firing rate curve without relying upon topographical inputs (Lengyel et al. 2003; O'Keefe and Recce 1993). It proposes that the firing probability of a place cell is determined by the amplitude of the summation or composite oscillation of two sinusoids with slightly different frequencies within a place cell. The envelope oscillation is unimodal in shape and, therefore, can mimic the firing rate curve tuning in recordings. Since they predict a repeating series of firing fields rather than a single one, additional mechanisms must be posited to account for the absence of out-of-field firing in place cells as pointed in O'Keefe and Burgess (2005).

In this paper, we try to find intrinsic properties of place cells dominating the unimodal tuning of firing rate, avoiding relying upon topographical inputs. We propose a working hypothesis that the coupling of dendritic with the soma–axonal action potential initiation zone of CA1 pyramidal cells is neuron's activity-dependent, and the weakest coupling happens around the center of a place field. The essential idea of our hypothesis is based on recently accumulated observations on variable or activity-dependent forward and back propagation in CA1 pyramidal neurons (Gasparini et al. 2004; Golding et al. 2001; Golding and Spruston 1998; Hoffman and Johnston 1999; Hoffman et al. 1997; Jarsky et al. 2005; Johnston et al. 1999; Migliore et al. 2005; Pan and Colbert 2001). The hypothesis is embodied in a reduced two-compartment model of CA1 neurons (Kamondi et al. 2002) by attaching a regulable feature to the coupling conductance parameter that is usually thought to be constant. Computer simulations showed that the dynamically modifiable coupling conductance plays a critical role for the emergence of a unimodal profile of firing rate, which is independent from the generation mechanism for theta phase precession. The later is induced by a slight difference in frequency of subthreshold oscillations of membrane potentials between two compartments, whose basic idea is proposed in previous modeling studies (Booth and Bose 2001; Bose et al. 2000; Bose and Recce 2001; Lengyel et al. 2003; O'Keefe and Recce 1993). Results accord with electrophysiological data on the separation between the temporal and rate property of spiking pattern (Huxter et al. 2003). Moreover, our model agrees well with observation that phase precession persists after transient silence of hippocampus activity (Zugaro et al. 2005).

2 Working hypothesis

There are two action potential initiation zones in pyramidal neurons, into which the studies of CA1 hippocampal and layer V neocortical pyramidal neurons have offered insights, especially. One is at the soma–axon where action potentials are generated and usually propagate actively back into the dendritic trees. Another zone is located in the dendrites, where regenerative voltage spikes can be initiated under certain conditions and propagate to soma. The presence of the initiation zone of apical dendrites has led to the suggestion that the pyramidal neuron has two functional compartments (Mainen and Sejnowski 1996; Pinsky and Rinzel 1994; Spencer and Kandel 1961; Yuste et al. 1994). The connection between two compartments is modeled by an axial resistance with a constant conductance that causes current to enter or leave the compartments. The coupling is generally thought to describe the passive propagation of current flows that flow back-and-forth between somatic and dendritic compartments and therefore assumed to be constant for a given type of neurons (Kamondi et al. 1998; Kepecs et al. 2002; Mainen and Sejnowski 1996; Pinsky and Rinzel 1994). Having a limited number of variables and parameters, the reduced two-compartment models are endowed with a powerful ability for exploring the essential properties of pyramidal neurons. However, according to recent evidences summarized as follows, we are inspired to reconsider whether it is reasonable to mimic the coupling interaction as constant within a behavior timescale of about 1 or 2 s, during which the animal traverses a place field.

Anatomically the dendritic action potential initiation zone is connected with the axonal initiation zone by a long part of

the main apical trunk and oblique dendrites that are situated in the proximal apical dendritic region and constitute a big part of the apical tree surface. Functionally, this region acts and contributes to the neuron firing as a coupling zone (Larkum et al. 2001). For CA1 pyramidal cells, it represents the main target of excitatory synaptic inputs from CA3 Schaffer collaterals, in contrast to the distal tuft dendrites that receive inputs from the perforant path (Spruston 2008). Accumulated observations show that the suprathreshold signal propagation between two initiation zones of CA1 pyramidal neurons can be pronouncedly modulated in this coupling zone by local properties such as membrane potential and active conductances. Let us first focus on forward propagation. The extent of dendritic spike propagation to soma is found to be variable (Golding and Spruston 1998). The effective invasion of the soma/axon region by the dendritic spikes is easily modulated by physiological relevant parameters such as the dendritic membrane potential and interactions with transient depolarization in dendrites (Gasparini et al. 2004), the availability of A-type K^+ channels in dendrites (Hoffman et al. 1997), and synaptic activity from the Schaffer collaterals (Jarsky et al. 2005). Especially, a clear gate modulation of forward propagation of dendritically evoked Na^+ spike by Schaffer-collateral synapses is shown recently (Jarsky et al. 2005). Dendritic spikes induced by strong perforant-path excitatory activation to the distal apical dendritic tuft could fail to propagate to the soma due to the long distance between inputs and the soma. Limited activation of CA1 neurons by perforant path, however, can be greatly facilitated by modest activation of Schaffer-collateral synapses in basal and proximal apical dendrites (Jarsky et al. 2005). Above data display that forward propagation of dendritic spikes can be effectively attenuated or boosted depending on the physiologically relevant factors along the somatodendritic axis. Similar to the modulation of forward-propagation signal, back-propagating action potentials can also be regulated dynamically by several factors in the coupling zone. Combining cell recordings with theoretical approach by using realistic computational models of CA1 pyramidal cells, previous studies demonstrate that the distribution, density, or modulatory state of Na^+ and A-type K^+ channels in the dendrites are important factors controlling the switch between strong and weak back-propagation of action potentials (Golding et al. 2001; Hoffman et al. 1997; Johnston et al. 1999; Migliore et al. 2005; Pan and Colbert 2001). Even subtle changes in the distribution of Na^+ and A-type K^+ channels along the somatodendritic axis can induce a dichotomy of action potential propagation (Golding et al. 2001). The rapid modulation by A-type K^+ channels is upon membrane depolarization and several neurotransmitters such as β-adrenergic and muscarinic acetylcholine receptors, whose activation is through PKA and PKC (Hoffman and Johnston 1999). Interestingly, β-adrenergic and muscarinic acetylcholine receptors have levels in the stratum radiatum of CA1 (Adem et al. 1997; Booze et al. 1993), a localization just between somatic and dendritic compartment, i.e., just within the coupling zone.

These evidences support that the coupling currents that flow back-and-forth between somatic and dendritic action potential initiation zone in CA1 pyramidal cells are not passively propagated but easily regulated depending on the neuron's activities. It is in contrast to two-compartment models that neither distinguish proximal apical dendrite from apical dendritic tuft as a modulating gate of signal propagation nor involve transient A-type potassium channels that are actually abundant in CA1 dendrites. Therefore, we hypothesize that the coupling term in originally proposed two-compartment model of CA1 place cells (Kamondi et al. 1998; Kepecs et al. 2002; Pinsky and Rinzel 1994) is not constant but neuron's activity-dependent during a sustained activity period like traversal process of a place field, and the weakest coupling happens around the center of a place field. Although current evidences summarized above are not detailed enough to provide a clear image about how the coupling is specifically regulated as a place field is crossed, the occurrence of the weakest coupling around the field center in our working hypothesis is consistent with theoretical analysis showing a tight relation of bursting occurrence with an intermediate range of electronic coupling conductance (Mainen and Sejnowski 1996; Pinsky and Rinzel 1994). Note a consistency between a high probability of bursting in a place cell and high frequency firing around its field center. Moreover, extracellular recordings within freely behaving animals discover that the spike amplitude decreases as animal runs through the place field (Quirk et al. 2001). While it seems to imply a monotonical decrease in the coupling between somatic and dendritic compartment after the animal enters a place field, the small tail going up in Fig. 2b in Quirk et al. (2001) shows the complexity of signal propagation modulation in CA1 pyramidal cells. The specific realization of our working hypothesis on a modulated coupling is explained in next Section.

3 Methods

3.1 Two-compartment neuron model

We simulate a CA1 place cell by using a two-compartment model described in Kamondi et al. (1998) and Kepecs et al. (2002). The model is minimal for reproducing spikes as well as bursts in a pyramidal cell, with one compartment representing the lumped soma and axon and another representing dendritic part. The somatic compartment includes sodium and potassium currents I_{Na} and I_K, respectively, while the dendritic compartment contains a persistent Na^+ current I_{NaP} and a voltage-gated slowly activating K^+ current I_{KS}. The current balance equations are given as follows:

$$C_m \dot{V}_s = -I_{Leak} - I_{Na} - I_K + \frac{g_c}{p}(V_d - V_s) + I_s, \quad (1)$$

$$C_m \dot{V}_d = -I_{Leak} - I_{NaP} - I_{KS} + \frac{g_c}{1-p}(V_s - V_d) + I_d, \quad (2)$$

where I_{Leak} is the leak current, and I_s and I_d are the injected currents separately applied to the soma and dendrite that will be explained in detail in another Subsection below. C_m is the capacitance density with $C_m = 1\mu\text{F/cm}^2$. The somatic and dendritic membrane potentials are denoted by V_s and V_d in mV. The fourth term in the right hand of each equation describes the current flow between compartments, whose formula follows Kamondi et al. (1998) except the coupling conductance g_c is endowed with a property of modifiability. The reason for introducing a modified g_c is based on our working hypothesis and demonstrated in detail in next Subsection. Parameter p measures the ratio of two compartment areas by setting p = somatic area/total area with $p = 0.15$ in simulations.

The voltage-dependent ionic currents are described by the standard Hodgkin–Huxley formalism. The kinetics of a gating variable x satisfies the first-order kinetics $dx/dt = \phi_x(\alpha_x(1-x) - \beta_x x) = \phi_x(x_\infty - x)/\tau_x$ where ϕ_x denotes the temperature scaling factor. All currents are expressed as current densities in $\mu\text{A/cm}^2$. $I_{Na} = g_{Na} m_\infty^3 h(V - E_{Na})$, where $m_\infty = \alpha_m/(\alpha_m + \beta_m)$, $\alpha_m = -0.1(V + 31)/(\exp(-0.1(V + 31)) - 1)$, $\beta_m = 4\exp(-(V + 56)/18)$, $\alpha_h = 0.07\exp(-(V + 47)/20)$, and $\beta_h = 1/(\exp(-0.1(V + 17)) + 1)$. $I_K = g_K n^4(V - E_K)$, where $\alpha_n = -0.01(V + 34)/(\exp(-0.1(V + 34)) - 1)$ and $\beta_n = 0.125\exp(-(V + 44)/80)$. $I_{NaP} = g_{NaP} r_\infty^3(V - E_{Na})$, where $r_\infty = 1/(\exp(-(V + 57.7)/7.7) + 1)$. $I_{KS} = g_{KS} q(V - E_K)$, where $q_\infty = 1/(\exp(-(V + 35)/6.5) + 1)$ and $\tau_q = 200/(\exp(-(V + 55)/30 + \exp((V + 55)/30))$. And $I_{Leak} = g_{Leak}(V - E_{Leak})$. The temperature factors are $\phi_h = \phi_n = 3.33$ and $\phi_q = 0.7$. The maximal conductance densities (in mS/cm^2) and the reversal potentials (in mV) are $g_{Na} = 45$, $g_K = 20$, $g_{NaP} = 0.09$, $g_{KS} = 0.9$, $g_{Leak} = 0.18$, $E_{Na} = +55$, $E_K = -90$, and $E_{Leak} = -65$.

3.2 Activity-dependent coupling between somatic and dendritic compartment

In Eqs. 1 and 2, coupling conductance g_c is a significant electronic parameter for determining model neuron's electrical structure. Although it cannot strictly and directly correspond to the specific parameters like core or axial conductances of Traub's cable model, g_c is usually thought to describe the passive propagation of current flows between somatic and dendritic compartments and therefore assumed to be constant for a given type of neurons (Kamondi et al. 1998; Kepecs et al. 2002; Pinsky and Rinzel 1994). The coupling term in the original form described in Eqs. 1 and 2 does not involve a dynamic or activity-dependent modifiability.

Unlike previous two-compartment models, our hypothesis assumes a dynamic coupling between dendritic and the somatic compartment in a CA1 place cell with the weakest coupling around the center of its place field. To embody the hypothesis in a simplest way and to keep the model's original style to an extent as great as possible, we only revise parameter g_c in Eqs. 1 and 2 from constant to be changeable. For simplification, a general U-shaped function versus position with the minimum value around field center is assumed for parameter g_c. Thus in such a revised model, as the animal traverses a place field the coupling conductance gradually decreases until around the center of field, then it gradually recovers to previous level when the animal approaches the end of the field.

It should be emphasized that the modifiable coupling conductance g_c assumed in our model does not mean that the passive axial conductance between soma and dendrites are variable but is just a phenomenological mimicking of the regulable property of coupling between two initiation zones observed in recordings.

3.3 Somatic and dendritic inputs

Locomotor activities are always accompanied with theta waves in hippocampus in rat. Hippocampal theta oscillation is characterized by a gradual phase-shift with depth from the pyramidal layer to the distal apical dendrites (reviewed in Buzsáki 2002). Simultaneous recordings of extracellular EEG activity in the CA1 pyramidal layer and intradendritic or intrasomatic activities of CA1 pyramidal neurons showed that membrane potentials of the pyramidal neurons oscillate coherently with theta EEG. Theta rhythm generally hyperpolarizes the soma while it depolarizes the dendritic membrane simultaneously (Artemenko 1972; Fox 1989; Kamondi et al. 1998; Leung and Yim 1986; Ylinen et al. 1995). The effect of theta rhythm drive on the cell membrane displays a gradual change along the length of the cell. Subthreshold oscillation of distal dendritic membrane potential has a frequency within theta band and is in antiphase with somatic subthreshold oscillation (Kamondi et al. 1998). In addition, a self-sustained dendritic oscillation can be induced in the theta frequency range by strong depolarization, even in the absence of extracellularly recorded theta activity (Kamondi et al. 1998). More recent study also supports the idea of two spatially segregated theta oscillators in soma and dendrites in CA1 pyramidal neurons (Hu et al. 2009).

Based on these evidences, two oscillations with slightly different frequencies were introduced to two compartments in previous studies to mimic in vivo state (Burgess et al. 2007; Lengyel et al. 2003). Similarly, we inject two out-of-phase sinusoidal currents I_s and I_d to the somatic and dendritic compartment, respectively, to simulate the inputs during exploratory behavior:

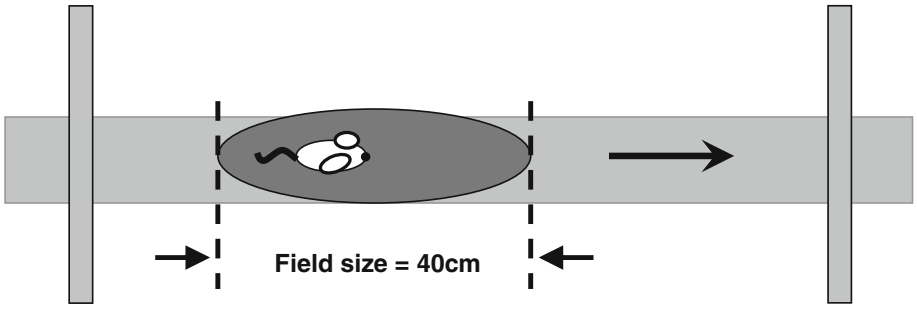

Fig. 1 Behavior task scheme. Rat moves unidirectionally along linear track with a place field

$$I_s = a_s \sin(2\pi f t) \tag{3}$$

$$I_d = b(v) + a_d \sin\left[2\pi(f + \Delta f(v))t + \pi\right]. \tag{4}$$

Parameters a_s and a_d are amplitudes of sinusoidal currents that by themselves are not sufficient to bring the cell to reach the firing threshold. Frequency f ranges within the theta rhythm band.

A difference from models by Lengyel et al. (2003) and Burgess et al. (2007) is the introduction of a speed-dependent current input $b(v)$ in Eq. 4, where v denotes the running speed. The DC component $b(v)$ is superimposed on the background theta and can push the place cell to a depolarization state depending on speed when animal enters a place field (Huhn et al. 2005). Actually the depolarization level of CA1 place cells is related to several behavior parameters, but to date the exact controlling relationship is unclear except animal's running speed. Running speed affects firing rate much more prominently than other behavior parameters do (Ekstrom et al. 2001; Huxter et al. 2003; McNaughton et al. 1983), although it is noted that overall its correlation with the firing rate varies among cells and is not high (Huxter et al. 2003). For simplification, we do not fabricate a specific function $b(v)$ but generally assume that $b(v)$ monotonically increases with v. Furthermore, dendritic depolarization by input $b(v)$ is hypothesized to induce an increase in the frequency of dendritic oscillation from f to $f + \Delta f(v)$, where $\Delta f(v)$ is an amount much smaller than f. This is supported by observations on voltage dependent changes in dendritic oscillation with higher frequencies responding to higher levels of depolarization in vivo (Kamondi et al. 1998). Similarly we do not go deep into the specific formula of $\Delta f(v)$ but emphasize its monotonically increasing property with v.

It is set $b(v) = 0$ and $\Delta f(v) = 0$ when animal leaves the place field.

3.4 Behavior parameters and data analysis

Only uniform motion is considered for simplification. The rat is assumed to unidirectionally traverse a place field with a constant speed v. Place field size is denoted by L and set as $L = 40\,\text{cm}$ in all simulations.

Instantaneous firing rate of the model neuron is calculated by dividing the number of spikes in a time window up to one theta cycle on either side of the reference spike by the size of the window. Spike phase is computed with respect to the troughs of the sinusoidal current injection to somatic compartment, defined as the phase origin 0° corresponding to the maxima of inhibition in model neurons.

4 Results

4.1 Separate mechanisms for generating unimodal firing rate tuning and monotonic spike phase precession

Consider that the animal moves across a place field with uniform velocity (Fig. 1). Our working hypothesis proposes that the unimodal profile of firing rate is generated by a mechanism totally different from that underlying the monotonic phase shift of spikes in place cells. The later is induced by the interaction between two oscillators with slightly different frequencies as previously proposed (Lengyel et al. 2003; O'Keefe and Recce 1993), whereas the former originates from the non-constant coupling between axo–soma and dendritic part.

Let us first check whether a non-constant coupling regulates firing rate profile during rat's passage along the field. A U-shaped coupling conductance that decreases and increases as the animal approaches and leaves the field center, respectively (Fig. 2b), is used to simulate a modifiable soma–dendrite interaction, as explained in Sect. 3. By a large amount of simulations we find that such a modifiable coupling does greatly regulate the firing rate. A U-shaped coupling conductance induces a highest firing rate around the field center and much lower firing rates in the periphery (Fig. 2e), which is consistent with the experimental recordings of firing patterns in place cells.

As shown in Fig. 2 the unimodal profile of firing rate is mainly due to a change in firing pattern (from single spikes to bursts) and an increase in spikes per burst towards the middle of the firing field. Why the change in coupling produces such an effect can be explained intuitively by partial electrical coupling of fast and slow currents spatially segregated. The somatic compartment includes only the classic

Hodgkin–Huxley channels necessary for spike generation, while the dendritic one contains currents responsible for bursting: a slowly activating potassium current, I_{KS}, and a fast-activating, persistent inward current, I_{NaP}. Too weak coupling leads to uncoupled case, in which the fast somatic- and slow dendritic subsystem fire independently and no isolated subsystem can burst. Very large coupling strength actually merges the two compartments into a single whole

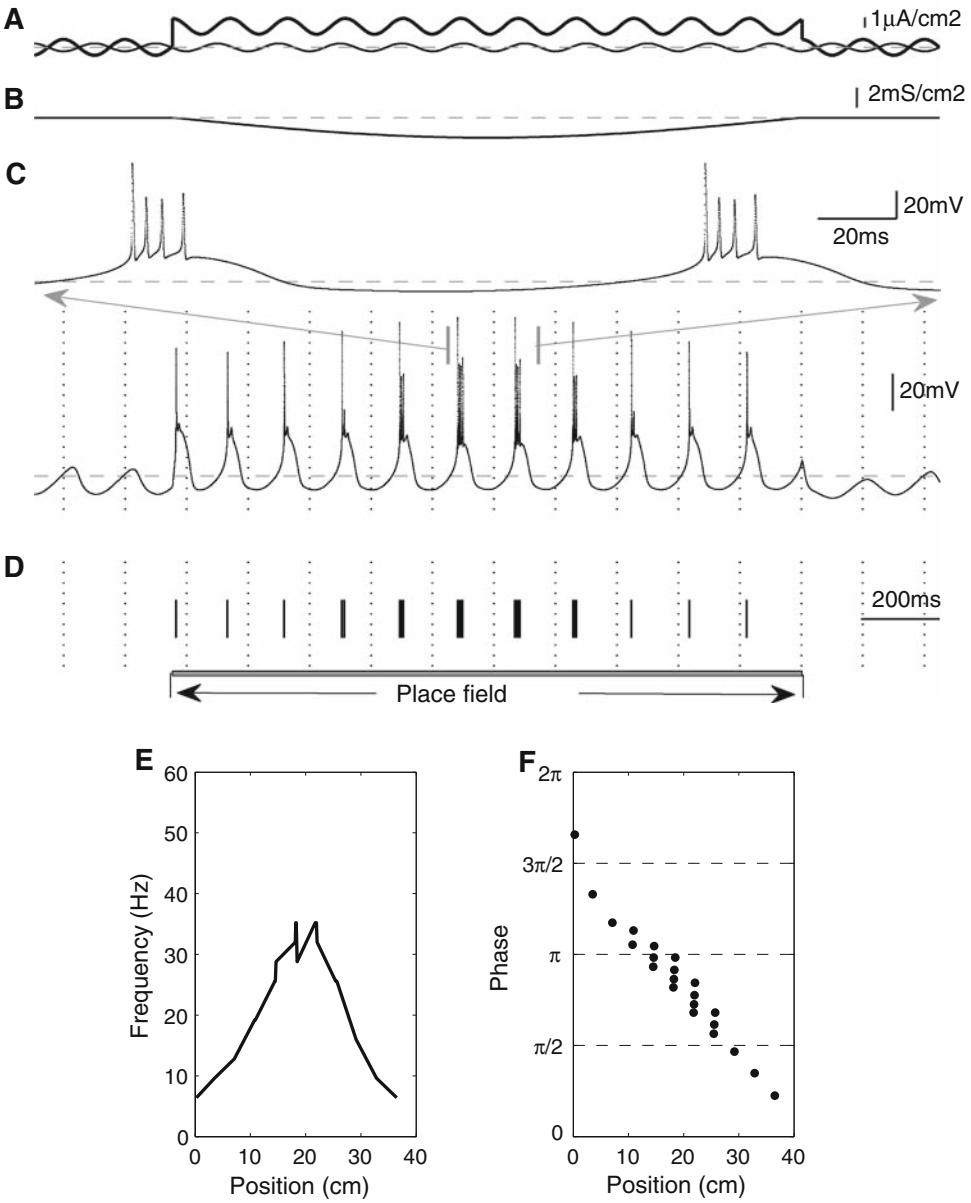

Fig. 2 Generation of unimodal firing rate profile and monotonic phase shift of spikes in a model CA1 place cell. Running speed is $v = 25$cm/s and place field size is $L = 40$cm. **a** Sinusoidal current injection to the soma $I_s = a_s \sin(2\pi f t)$ with $f = 6.4$Hz and $a_s = 0.4\mu\text{A}/\text{cm}^2$ (*thin curve*) and current input to the dendrite $I_d = a_d \sin[2\pi(f + \Delta f)t + \pi] + b$ with $a_d = 0.8\mu\text{A}/\text{cm}^2$, $\Delta f = 0.42$Hz, and $b = 2.1\mu\text{A}/\text{cm}^2$ (*thick curve*). Note $\Delta f = 0$ and $b = 0$ when the animal is outside the place field. *Horizontal long − dashed* line represents zero current level. **b** Coupling conductance with a U-shape regulation until the animal leaves place field. *Horizontal long − dashed* line represents $3\text{mS}/\text{cm}^2$. **c** Bottom: somatic membrane potential trace of the model place cell whose firing is constrained within the place field in a single traversal. The segment between two vertical bars is enlarged in the top trace. *Horizontal long-dashed* lines represent −60 mV voltage level. *Dotted lines* mark 0° or 360° for each theta rhythm cycle. **d** The same plot as that in the bottom trace of **c** except that spikes and bursts are represented by short ticks. Horizontal bar at the bottom marks the period for the rat to travel in place field. The time scale applies to all panels except the top trace of **c**. **e** Firing rate as a function of animal's position within place field. **f** Spike phase as a function of animal's position within place field. Each dot denotes a spike. Data in **e** and **f** are derived from **c**

(fully coupled) and does not allow bursts, too. Our model involves a moderate or intermediate coupling, which is shown to be suitable for producing a full range of firing patterns including bursts (Pinsky and Rinzel 1994). Bursting depends on a proper current reverberating between fast and slow subsystem, which is determined by the coupling strength. With the decrease of coupling conductance, the neuron model successively fires single spikes, doublets, and bursts with an increasing number of spikes, as explained in detail by the following example. It is consistent with some qualitative analysis about the effect of the coupling strength (Kepecs and Wang 2000; Pinsky and Rinzel 1994).

A representative example for a model place cell is shown in Fig. 2. The sinusoidal current input to soma has no change no matter whether the animal is within the field or not, which simulates a relatively stable inhibitory theta input (Fig. 2a). Dendritic compartment receives a sinusoidal current that is in antiphase with the somatic oscillation (Fig. 2a), which only induces a subthreshold oscillation by itself. Once entering the place field, an excitatory input $b(v)$ increasing with running speed is superimposed to dendrite (see Fig. 2a) making the place cell reach firing threshold (Fig. 2c). In accord with recordings in vivo, model neuron with a U-shape coupling regulation emits single spikes once the animal just enters the place field and discharges bursts in the field center and single spikes again in the late part of field (Fig. 2c). The number of spikes within individual bursts (called the length of a burst) progressively increases and decreases as the animal approaches and leaves the field center (Fig. 2c, d, f). In addition, our simulations reveal that the maximum firing rate is determined by the modulation depth of coupling conductance. The deeper g_c is modulated, the longer the maximum length of the bursts has (data not shown).

On the other hand, due to a slight difference in frequencies between two oscillators, the cycles of the faster oscillator occur progressively earlier relative to those of the slower one. It makes the phases of spikes happening on the strongest depolarization interval of each cycle steadily precess to earlier phases of theta cycles (Fig. 2c, d, f), as already described in previous studies on phase precession generation (Lengyel et al. 2003; O'Keefe and Recce 1993). A proper frequency difference $\Delta f(v)$ is critical to phase precession. A large amount of our simulations find that its value should be tightly related to field size and animal's running speed. If the rat runs straight along a field with size L at constant speed v, $\Delta f(v)$ should be proportional to v/L in order to ensure a total phase shift of 2π during a single traversal. This result confirms previous modeling studies (Burgess et al. 2007; Lengyel et al. 2003).

To further illustrate the separation of two characteristics in place cell firing, we hold $\Delta f(v) = 0$ but permit g_c to change as a U-shaped function within place field. Simulations show that a unimodal profile of firing rate occurs

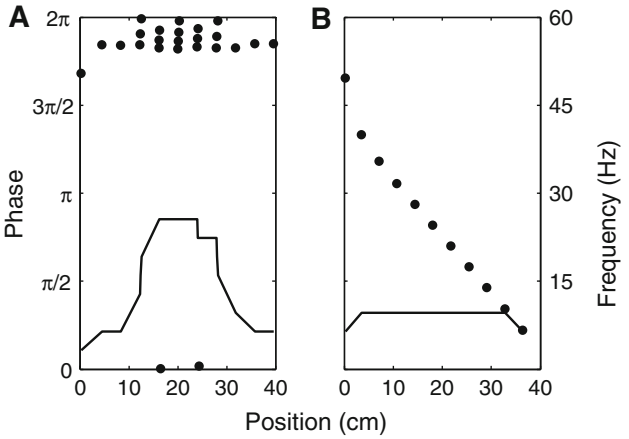

Fig. 3 Independence of the unimodal property of firing rate from spike phase precession. Values of all parameters in the model neuron are the same as those in Fig. 2 except Δf and g_c. Firing rate and spike phase are illustrated in the same single plot, where left axes of each plot express phase variable and the right axes denote frequency. **a** The unimodal profile of firing rate remains but the spike phase precession is totally damaged with parameters $\Delta f = 0$ and g_c changing exactly as shown in Fig. 2b. **b** Perfect phase precession but invalid firing rate coding with parameters $\Delta f = 0.42$Hz and $g_c = \text{constant} = 3\text{mS/cm}^2$

in modal neuron, but it is in company with constant spike phase across the whole field (Fig. 3a). On contrast, a constant g_c and a slightly frequency difference between dendritic and somatic oscillator give phase precession uniformly covering 2π but together with a quite flat firing rate curve (Fig. 3b).

Finally it needs to distinguish the effects of dendritic excitation from those of compartment coupling on the modulation of cell firing rate. The former, being assumed to monotonously increase with animal's speed, controls the level but not the profile of firing rate curve, as shown in Fig. 4. Whereas the extent of soma–dendrite coupling regulation is essential for inducing a unimodal profile of firing rate, no matter whether speed is constant or not. Of course, higher speed during a variable motion traversal also contributes to the formation of unimodal rate profile, but it cannot be the dominating cause. Otherwise, we cannot explain why the unimodal profile putatively exists in place cell firing, no matter whether the highest running speed appears in the field center or not.

4.2 Phase precession takes place equally on trials with low as well as high firing rate

Above results support that two mechanisms, respectively, for firing rate and phase precession are independent of each other. Then, a direct prediction comes to us that spike phase precession should occur even when the firing rate in place cells is very low, as shown by experimental evidences in Huxter et al. (2003). To examine this prediction, we simulate low firing rate trials by considerably decreasing the magnitude of

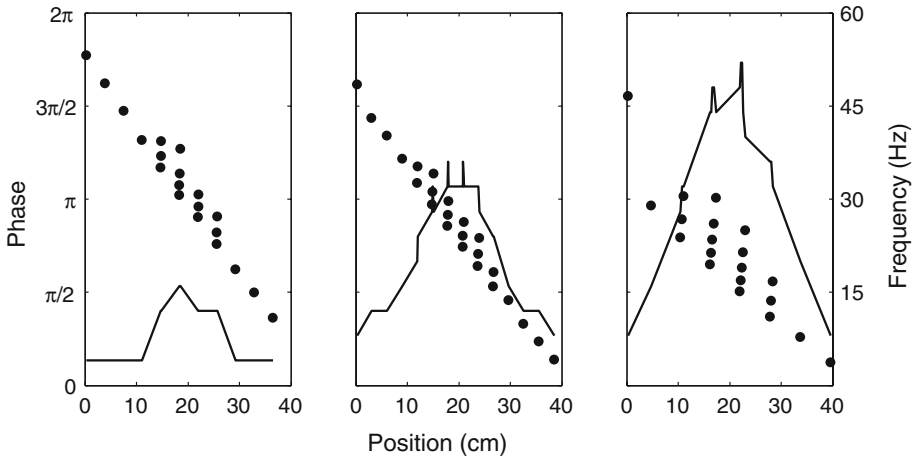

Fig. 4 Magnitude of dendritic excitation modulates the whole level but not the unimodal property of the position verse firing rate curve. Theta rhythm frequency is set as $f = 8$Hz, and other parameters are the same as that in Fig.2 except Δf and dendritic excitation magnitude b that vary as functions of speed v. Left: $v = 15$cm/s, $b = 0.7\mu$A/cm^2 and $\Delta f = 0.3$Hz. Middle: $v = 25$cm/s, $b = 2.0\mu$A/cm^2 and $\Delta f = 0.48$Hz. Right: $v = 50$cm/s, $b = 4.0\mu$A/cm^2 and $\Delta f = 0.6$Hz

dendritic excitation. Results are shown in Fig. 5. Apparently even if only a few spikes are emitted during single trials, these spikes still continuously precess to an earlier phase as in normal traversals. Results have a good agreement with experiment (Huxter et al. 2003).

4.3 Phase precession persists after transient silence perturbation of hippocampal activity

In this section, we check the model by examining the effect of transient silence perturbation on phase precession, whose design is inspired by recent report by Zugaro et al. (2005).

The advantage of modeling approach is the ability to overcome the hard constraints of in vivo methods. Delicate experiments in vivo by Zugaro et al. (2005) can be easily repeated by computer simulations in our model. Specifically, during the traversal along the place field, we transiently shut down the model neuron activity by holding $I_s = 0$ and $I_d = 0$ for 250 ms and reset the phase of theta rhythm by adding a randomly valued phase shift $\Delta\phi$ to the somatic sinusoidal current as $I_s = a_s \sin(2\pi f t + \Delta\phi)$ after activity recovery (i.e., after 250 ms). Note here that we implicitly assume that dendritic compartment's phase is not affected by this phase resetting. Such a perturbation is found to strongly alter the relationship between spike phase and spatial position, as shown in Fig. 6a, c. It is consistent with predictions of many two-oscillator models of phase precession according to Zugaro et al. (2005). However, if we also reset the phase of dendritic oscillator by the same amount $\Delta\phi$ as somatic oscillator simultaneously, i.e., $I_d = b(v) + a_d \sin[2\pi(f + \Delta f(v))t + \pi + \Delta\phi]$, as shown in Fig. 6b, phase precession is preserved after perturbation (Fig. 6d). Furthermore, our simulations show that the specific value of randomly resetting phase $\Delta\phi$ has no effect on the immediate recovery of phase precession (Fig. 7). Substantial levels of Gaussian noise are imposed on current $b(v)$ or both current $b(v)$ and reset phase $\Delta\phi$ of dendritic input I_d to mimic physiologically noisy stimuli in place cell. It is found that even with strong background noises phase precession still resumes robustly after transient silence perturbation (Fig. 8).

There are two causes for resumption of phase precession. One is the simultaneous resetting of both dendritic and somatic compartments' phase as explained above. Another is that phase difference between somatic and dendritic oscillator is not damaged by transient silence perturbation. The phase difference evolves from $\delta\phi_1^{d-s} = 2\pi\Delta f t_1 + \pi$ at instant time t_1 just before perturbation to $\delta\phi_2^{d-s} = 2\pi\Delta f t_2 + \pi$ with $t_2 = t_1 + 250$ ms upon neuron activity recovery. Here $\delta\phi^{d-s}$ is calculated by subtracting the phase of somatic oscillator from that of dendritic oscillator. Thus, phase precession is guaranteed to resume as if phase resetting and silence perturbation are never applied to the model. Based on this modeling, we predict two points about the experiment by Zugaro et al. (2005). One is that the phase resetting of subthreshold oscillation occurs not only in somatic, but also in dendritic membrane potential by the same amount. This is not a "miracle" but physiologically quite feasible, because soma and dendrites are tightly packed in the same neuron. Otherwise, it is odd enough if the phase resetting of theta oscillations affects only soma but not dendritic compartment. Second, neither the antiphase relationship nor the frequency difference between two oscillators is violated by the perturbation. These predictions need to be examined by neurophysiologic recordings in future.

5 Discussion

5.1 Comparison with related models on dual coding in place cells

A variety of different models have been developed to account for mechanisms underlying dual coding in place cells, most of which consider dual coding inseparable. Several of these

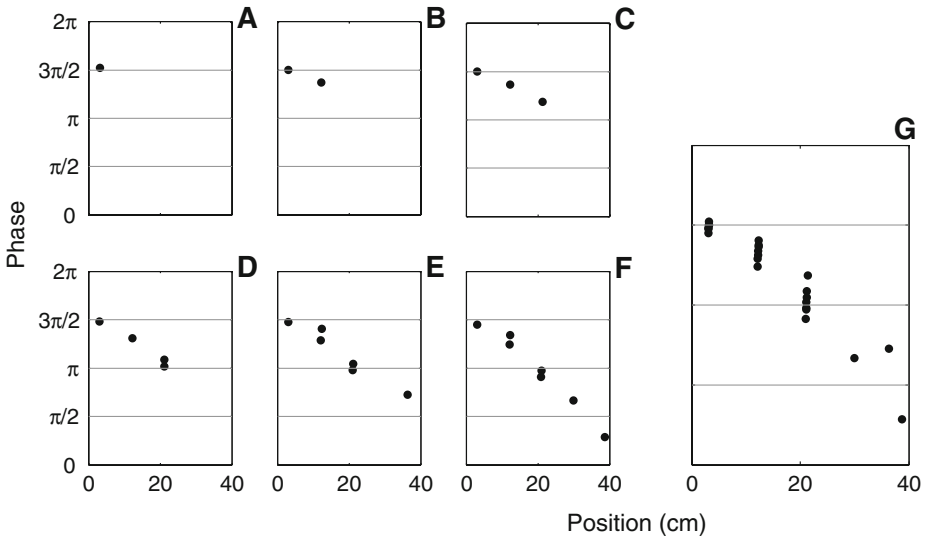

Fig. 5 Spike phase continuously advances to earlier phase on low as well as high firing rate runs. Parameters are set as $f = 8$Hz, $v = 25$cm/s, and $\Delta f = 0.52$Hz, and other parameter values are the same as that in Fig.2 except dendritic excitation magnitude b. (**a**–**f**) Phase precession occurs on individual six runs with b, respectively, taking a value in the range from 0.05 to 0.2μA/cm^2. From **a** to **f**, the value of parameter b increases successively. All the data of six runs in panels **a** to **f** are pooled together in the right panel **g**

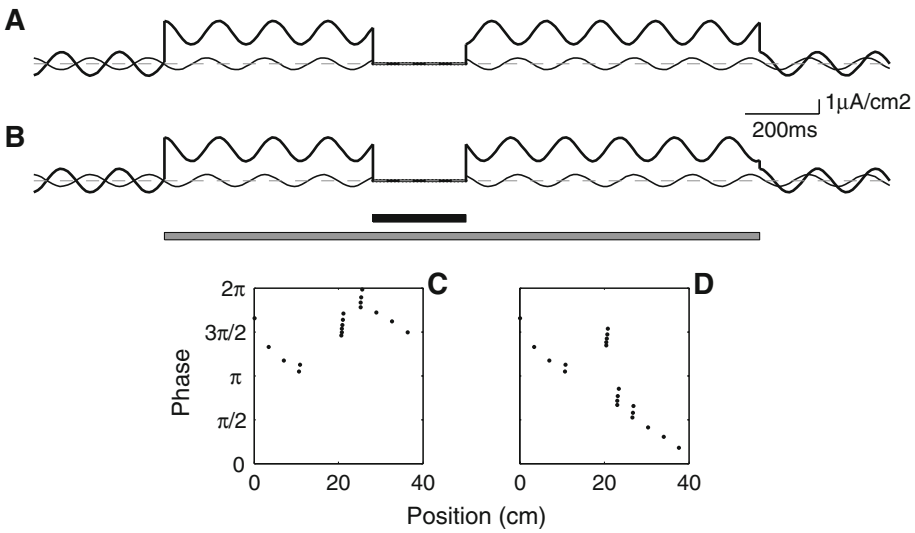

Fig. 6 The correlation between spike phase and animal's spatial position after hippocampus discharge is transiently turned off for 250 ms and theta rhythm phase is randomly reset. Each parameter of the model neuron takes the same value as that in Fig. 2 except that during transient silence perturbation $I_s = 0$, $I_d = 0$, and theta rhythm phase is reset. **a** Sinusoidal current injection to the soma (*thin curve*) and current input to the dendrite (*thick curve*). *Horizontal long-dashed* line represents zero current level. The phase of theta rhythm is reset after 250 ms by setting parameter $\Delta\phi = 1.3\pi$ for somatic sinusoidal current (see text for the meaning of $\Delta\phi$). **c** Perturbation in **a** strongly damages the phase-position relationship. **b** and **d** are the same as **a** and **c**, respectively, except the phase of dendritic current input is also reset simultaneously with somatic oscillator with the same phase shift $\Delta\phi = 1.3\pi$. Phase precession continues after perturbation in **d**. Long horizontal bar at the bottom of **b** marks the period for the rat to travel in place field, and the short one denotes the 250 ms period for silence perturbation

models assume increasing amounts of excitation input to dendrite by combining somatic inhibition in place fields (Harris et al. 2002; Kamondi et al. 1998; Magee 2001; Mehta et al. 2002). Another one considers the effect of synaptic inhibition on burst firing (Booth and Bose 2001). As for interference model (Lengyel et al. 2003; O'Keefe and Burgess 2005; O'Keefe and Recce 1993), the firing probability of a place cell is determined by the amplitude of the composite oscillation of two sinusoids with slightly different frequencies. While the interference model has a great potential to underlie the grid-like firing pattern of entorhinal grid cells and successfully predicts the existence of phase precession in these cells (Burgess et al. 2007; Hafting et al. 2008; O'Keefe and Burgess 2005), one problem arises when it is applied to place cells. It predicts a repeating series of firing fields rather than a single one.

It is interesting to check whether the basic interference effect is also present in our model. By removing the DC

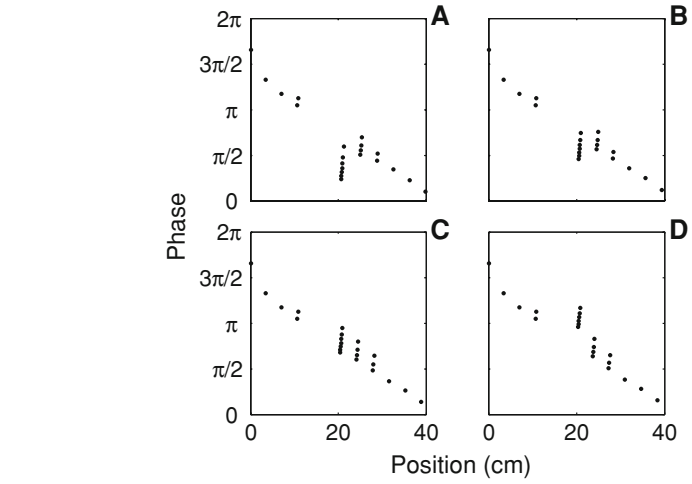

Fig. 7 Specific value of randomly resetting phase $\Delta\phi$ has no effect on the immediate recovery of phase precession after hippocampal silence perturbation. All parameters take the same values as that in Fig. 6b except $\Delta\phi$. **a** $\Delta\phi = 0.1\pi$. **b** $\Delta\phi = 0.4\pi$. **c** $\Delta\phi = 0.65\pi$. **d** $\Delta\phi = 0.94\pi$. **e** The somatic membrane potential trace corresponding to **d**. *Dotted lines* mark 0° or 360° for each theta rhythm cycle. Note the change in theta rhythm phase marked by arrow head after perturbation

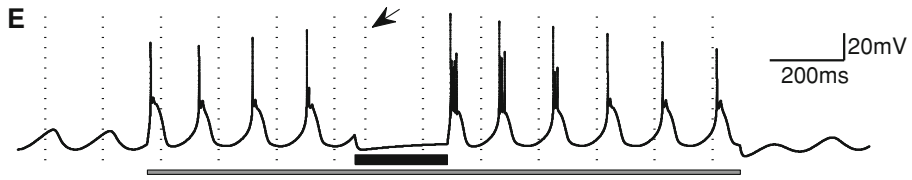

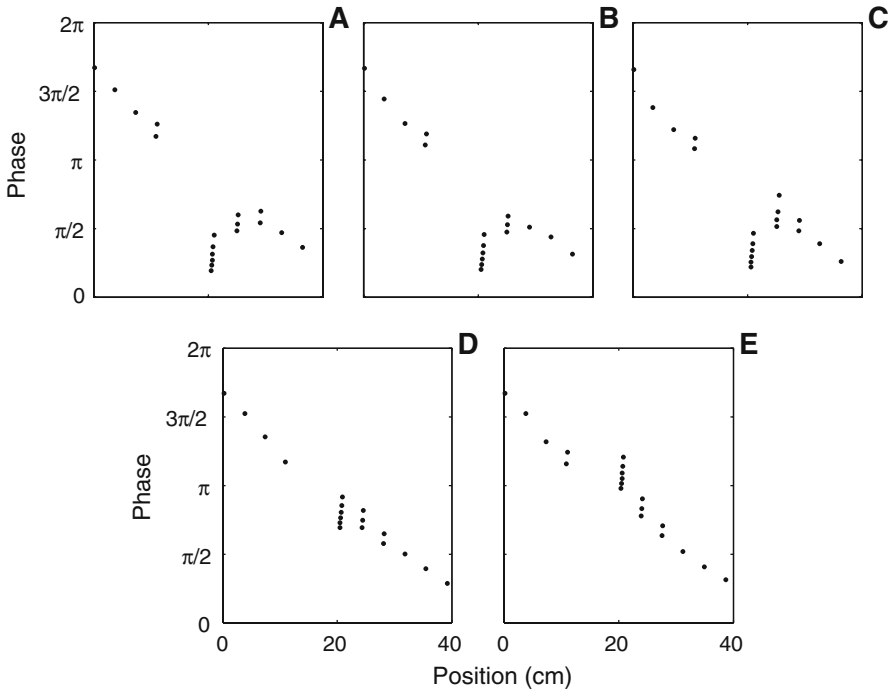

Fig. 8 Resumption of phase precession is noise against. **a**–**c** The current $b(v)$ of dendritic input is randomized with 30% **a**, 20% **b**, and 10% **c** Gaussian noise, respectively, and other parameters are the same as that in Fig. 7a. **d**-**e** Both current $b(v)$ and reset phase $\Delta\phi$ of dendritic input are randomized with 30% Gaussian noise, and other parameters in Fig. 8d and 8e take the same values as that in Fig. 7c and 7d, respectively

component from dendritic input and setting the coupling conductance as constant, we actually change our model into an oscillatory interference one. Many pairs of subthreshold sinusoidal currents, together with different constant coupling, are tried in simulations. However, all results show a quite weak difference between peak rates and rates in the field periphery, resulting in a nearly flat firing profile (data not shown). We reason that it might be due to the complex coding of bursting neurons. In contrast to a traditional Hodgkin–Huxley neuron firing at a rate proportional to input amplitude, a class of bursting neuron models including the current one do not show clear amplitude coding but signal the input slope (Kepecs et al. 2002). The amplitude profile of the composite oscillation in the interference model therefore could not be detected. Of course it does not rule out strong interference effect on neurons with different bursting mechanisms.

In a sum, in contrast to above models, our model suggests the independence of temporal coding from rate coding. On one hand, we adopt the key idea of previous models on phase precession: the cycles of the faster oscillator occur progressively earlier relative to those of the slightly slower oscillator (Lengyel et al. 2003; O'Keefe and Recce 1993). On the other hand, our model is distinct from others by basing the unimodal profile of rate coding on the intrinsic properties of place cells: neuron activity-dependent coupling between somatic and dendritic compartment. It should be noted that the model of Huhn et al. (2005) also decouples the phase and rate codes. But a quite different mechanism from ours is proposed: somatic depolarization only modulates firing rate, whereas dendritic inputs determine the spike phase.

An elegant study recently identified three subthreshold properties of CA1 place fields (Harvey et al. 2009). One is a ramp-like depolarization of the membrane potential, which is usually assumed to be induced by a ramp-like dendritic input. As we have discussed in Sect. 4 (about the effect of dendritic excitation on firing rate) and in this Section (about why the ramp-like amplitude profile of the composite oscillation in the interference model could not be detected by a class of bursting neurons), this property alone can not explain the unimodal profile of firing rate. A slightly faster intracellular theta oscillation than the extracellularly recorded theta rhythm, identified in Harvey et al. (2009), is exactly what our model describes. As for the last property of an increase in the amplitude of membrane potential theta oscillations, although it is not proposed in our model, its inclusion does not affect our final conclusions. It should be noted that as yet data by Harvey et al. (2009) is not enough to distinguish whether the dual coding is independent or not.

Skaggs et al. (1996) found that a non-liner regression like a banana shape between firing phase and rat's position fit data much better than a purely linear one did. Further analysis shows that it consists of two components (Yamaguchi et al. 2002). While the mechanism underlying the second component is difficult to be resolved yet, Yamaguchi (2003) accounts for the 180° linear phase advance by phase locking hypothesis among coupled neuron oscillators. Interestingly, phase locking can also appear in our model when frequency conditions are satisfied by two compartments (data not shown). But the probability of phase locking is low and it can only produce a total 180° phase precession.

A feature of phase precession in the model is a linear phase decrease. Actually data show a variety in recordings: the 360° linear (O'Keefe and Recce 1993; Zugaro et al. 2005) and the non-linear phase shift (Skaggs et al. 1996; Yamaguchi et al. 2002). We think that the argument about which kind of data is more exact or which model is correct may be misleading. First, there might exist two kinds of phase precession generators. One is individual pyramidal cells distributed in hippocampus itself, at least in CA1. Another is located in its upstream region, the entorhinal cortex superficial layers, where phase precession is generated and inherited by CA3 and CA1 (Burgess et al. 2007; O'Keefe and Burgess 2005; Yamaguchi 2003; Yamaguchi et al. 2007). It should be noted that the latter can also account for persistent phase precession in Zugaro et al. (2005). Second, phase precession may include two compositions generated by different dynamics: phase locking (Yamaguchi 2003) and the soma–dendritic inference as in this model. The ratio of two compositions might vary depending on recording conditions whose details are still unclear to us. We speculate upon that different sources of phase precession may play different roles in neural circuit underlying cognitive map.

5.2 Modifiable coupling in two-compartment neuron model

In our model, the modifiable coupling is assumed to experience an early loosing and late recovering process as rat moves through the place field. The weakest coupling occurs around the field center for simple illustration. Many other cases that the weakest coupling appears in non-field center position are also tried in our simulations. Results can explain the appearance of positively or negatively skewed place fields (Mehta et al. 2000) very well (data not shown), covering a variety of asymmetric field shapes observed in vivo.

For simplification, our model does not distinguish direction sensitivity of the coupling regulation: the U-shaped regulation curve is applicable to both antidromic (soma-to-dendrite) and orthodromic directions. Based on asymmetric intracellular factors like non-uniform channel density of a transient K^+ (Hoffman et al. 1997) and hyperlarization-activated I_h current (Magee 1998) across the antidromic axis, however, we infer that the strength of a "handshake" between spike-initiating zone in the axon and distal dendritic zones may be propagation direction specific. To our surprise, a more recent study published during the revision of the present one, indeed, shows that the propagation of subthreshold voltage signals between soma and dendrites is propagation-direction sensitive (Hu et al. 2009). Besides, such propagation is modulated by the state of the cell, including membrane potential, M- and h-channel density, and input frequency. These data by using subthreshold stimuli, as a complement to evidences on neuron activity-dependent propagation of evoked spikes, strongly support our hypothesis on the modifiable coupling.

Attaching a changeable property to the coupling conductance, as in our model, is only a phenomenological approach. From the viewpoint of modeling, it is necessary to compare it with another way proposed for layer 5 (L5) pyramidal neurons of the rat neocortex that are similar to CA1 neurons in architecture of dendrites (Larkum et al. 2001). To improve a L5 neuron model, a third compartment simulating the apical oblique dendrites is proposed to be inserted between original two compartments (Larkum et al. 2001). This compartment

controls the coupling between the other two. For CA1 pyramidal neurons, the oblique dendrites constitute the main target of Schaffer collateral axons from CA3, while the distal apical dendritic tuft receives distinct excitatory inputs from layer III of entorhinal cortex. Our results here support a necessity of expanding the reduced CA1 two-compartment model to a three-compartment one, in a similar way to L5 neuron modeling. The third compartment is expected to execute the function of a regulable coupling parameter in this study in some extent.

Acknowledgements We greatly thank Dr. Jinhui Wang and Dr. Naoyuki Sato for useful discussions. We also thank the reviewers for their constructive comments. The first author would express special thanks to Dr. Aike Guo for his continuous encouragement and discussions. The first author was supported by the Knowledge Innovation Engineering Project of Chinese Academy of Sciences (grant KSCX2-YW-R-39) and National Science Foundation of China (grants 30630028 and 30770495).

References

Adem A, Jolkkonen M, Bogdanovic N, Islam A, Karlsson E (1997) Localization of M1 muscarinic receptors in rat brain using selective muscarinic toxin-1. Brain Res Bull 44:597–601

Artemenko DP (1972) Role of hippocampal neurons in theta-wave generation. Neurophysiologia 4:409–415

Booth V, Bose A (2001) Neural mechanisms for generating rate and temporal codes in model CA3 pyramidal cells. J Neurophysiol 85:2432–2445

Booze RM, Crisostomo EA, Davis JN (1993) Beta-adrenergic receptors in the hippocampal and retrohippocampal regions of rats and guinea pigs: autoradiographic and immunohistochemical studies. Synapse 13:206–214

Bose A, Booth V, Recce M (2000) A temporal mechanism for generating the phase precession of hippocampal place cells. J Comput Neurosci 9:5–30

Bose A, Recce M (2001) Phase precession and phase-locking of hippocampal pyramidal cells. Hippocampus 11:204–215

Burgess N, Jackson A, Hartley T, O'Keefe J (2000) Predictions derived from modelling the hippocampal role in navigation. Biol Cybern 83:301–312

Burgess N, Barry C, O'Keefe J (2007) An oscillatory interference model of grid cell firing. Hippocampus 17:801–812

Buzsáki G (2002) Theta oscillations in the hippocampus. Neuron 33:325–340

Ekstrom AD, Meltzer J, McNaughton BL, Barnes CA (2001) NMDA receptor antagonism blocks experience-dependent expansion of hippocampal "place fields". Neuron 31:631–638

Fox SE (1989) Membrane potential and impedance changes in hippocampal pyramidal cells during theta rhythm. Exp Brain Res 77:283–294

Gasparini G, Migliore M, Magee JC (2004) On the initiation and propagation of dendritic spikes in CA1 pyramidal neurons. J Neurosci 24:11046–11056

Golding NL, Spruston N (1998) Dendritic sodium spikes are variable triggers of axonal action potentials in hippocampal CA1 pyramidal neurons. Neuron 21:1189–1200

Golding NL, Kath W, Spruston N (2001) Dichotomy of action-potential backpropagation in CA1 pyramidal neuron dendrites. J Neurophysiol 86:2998–3010

Hafting T, Fyhn M, Bonnevie T, Moser M, Moser E (2008) Hippocampus-independent phase precession in entorhinal grid cells. Nature 453:1248–1253

Harris KD, Henze DA, Hirase H, Leinekugel X, Dragoi G, Czurkó A, Buzsáki G (2002) Spike train dynamics predicts theta-related phase precession in hippocampal pyramidal cells. Nature 417:738–741

Hartley T, Burgess N, Lever C, Cacucci F, O'Keefe J (2000) Modeling place fields in terms of the cortical inputs to the hippocampus. Hippocampus 10:369–379

Harvey CD, Collman F, Dombeck DA, Tank DW (2009) Intracellular dynamics of hippocampal place cells during virtual navigation. Nature 461:941–946

Hoffman DA, Johnston D (1999) Neuromodulation of dendritic action potentials. J Neurophysiol 81:408–411

Hoffman DA, Magee JC, Colbert CM, Johnston D (1997) K^+ channel regulation of signal propagation in dendrites of hippocampal pyramidal neurons. Nature 387:869–875

Hu H, Vervaeke K, Graham L, Storm JF (2009) Complementary theta resonance filtering by two spatially segregated mechanisms in CA1 hippocampal pyramidal neurons. J Neurosci 29:14472–14483

Huhn Z, Orbán G, Érdi P, Lengyel M (2005) Theta oscillation-coupled dendritic spiking integrates inputs on a long time scale. Hippocampus 15:950–962

Huxter J, Burgess N, O'Keefe J (2003) Independent rate and temporal coding in hippocampal pyramidal cells. Nature 425:828–832

Jarsky T, Roxin A, Kath WL, Spruston N (2005) Conditional dendritic spike propagation following distal synaptic activation of hippocampal CA1 pyramidal neurons. Nat Neurosci 8:1667–1676

Johnston D, Hoffman DA, Colbert CM, Magee JC (1999) Regulation of back-propagating action potentials in hippocampal neurons. Curr Opin Neurobiol 9:288–292

Kamondi A, Acsády L, Wang X-J, Buzsáki G (1998) Theta oscillations in somata and dendrites of hippocampal pyramidal cells in vivo: activity-dependent phase-precession of action potentials. Hippocampus 8:244–261

Kepecs A, Wang X-J (2000) Analysis of complex bursting in cortical pyramidal neuron models. Neurocomputing 32–33:181–187

Kepecs A, Wang X-J, Lisman J (2002) Bursting neurons signal input slope. J Neurosci 22:9053–9062

Larkum ME, Zhu JJ, Sakmann B (2001) Dendritic mechanisms underlying the coupling of the dendritic with the axonal action potential initiation zone of adult rat layer 5 pyramidal neurons. J Physiol 533:447–466

Lengyel M, Szatmáry Z, Érdi P (2003) Dynamically detuned oscillations account for the coupled rate and temporal code of place cell firing. Hippocampus 13:700–714

Leung LS, Yim CY (1986) Intracellular records of theta rhythm in hippocampal CA1 cells of the rat. Brain Res 367:323–327

Lever C, Burton S, Jeewajee A, O'Keefe J, Burgess N (2009) Boundary vector cells in the subiculum of the hippocampal formation. J Neurosci 29:9771–9777

Magee JC (1998) Dendritic hyperpolarization-activated currents modify the integrative properties of hippocampal CA1 pyramidal neurons. J Neurosci 18:7613–7624

Magee JC (2001) Dendritic mechanisms of phase precession in hippocampal CA1 pyramidal neurons. J Neurophysiol 86:528–532

Mainen Z, Sejnowski TJ (1996) Influence of dendritic structure on firing pattern in model neocortical neurons. Nature 382:363–366

McNaughton BL, Barnes CA, O'Keefe J (1983) The contributions of position, direction, and velocity to single unit activity in the hippocampus of freely moving rats. Exp Brain Res 52:41–49

Mehta MR, Quirk MC, Wilson MA (2000) Experience-dependent asymmetric shape of hippocampal receptive fields. Neuron 25:707–715

Mehta MR, Lee AK, Wilson MA (2002) Role of experience and oscillations in transforming a rate code into a temporal code. Nature 417:741–746

Migliore M, Ferrante M, Ascoli GA (2005) Signal propagation in oblique dendrites of CA1 pyramidal cells. J Neurophysiol 94:4145–4155

O'Keefe J, Recce ML (1993) Phase relationship between hippocampal place units and the EEG theta rhythm. Hippocampus 3:317–330

O'Keefe J, Burgess N (2005) Dual phase and rate coding in hippocampal place cells: theoretical significance and relationship to entorhinal grid cells. Hippocampus 15:853–866

Pan E, Colbert CM (2001) Subthreshold inactivation of Na^+ and A-type K^+ channels supports the activity-dependent enhancement of back-propagating action potentials in hippocampal CA1 pyramidal neurons. J Neurophysiol 85:1013–1016

Pinsky PF, Rinzel J (1994) Intrinsic and network rhythmogenesis in a reduced traub model for CA3 neurons. J Comput Neurosci 1:39–60

Quirk MC, Blum KI, Wilson MA (2001) Experience-dependent changes in extracellular spike amplitude may reflect regulation of dendritic action potential back-propagation in rat hippocampal pyramidal cells. J Neurosci 21:240–248

Skaggs WE, McNaughton BL, Wilson MA, Barnes CA (1996) Theta phase precession in hippocampal neuronal populations and the compression of temporal sequences. Hippocampus 6:149–172

Solstad T, Boccara CN, Kropff E, Moser MB, Moser EI (2008) Representation of geometric borders in the entorhinal cortex. Science 322:1865–1868

Spencer WA, Kandel ER (1961) Electrophysiology of hippocampal neurons. J Neurophysiol 24:272–288

Spruston N (2008) Pyramidal neurons: dendritic structure and synaptic integration. Nat Rev Neurosci 9:206–221

Yamaguchi Y (2003) A theory of hippocampal memory based on theta phase precession. Biol Cybern 89:1–9

Yamaguchi Y, Aota Y, McNaughton BL, Lipa P (2002) Bimodality of theta phase precession in hippocampal place cells in freely running rats. J Neurophysiol 87:2629–2642

Yamaguchi Y, Sato N, Wagatsuma H, Wu Z, Molter C, Aota Y (2007) A unified view of theta-phase coding in the entorhinal-hippocampal system. Curr Opin Neurobiol 17:197–204

Ylinen A, Soltész I, Bragin A, Penttonen M, Sik A, Buzsáki G (1995) Intracellular correlates of hippocampal theta rhythm in identified pyramidal cells, granule cells and basket cells. Hippocampus 5:78–90

Yuste R, Gutnick MJ, Saar D, Delaney KR, Tank DW (1994) Ca^{2+} accumulations in dendrites of neocortical pyramidal neurons: an apical band and evidence for two functional compartments. Neuron 13:23–43

Zugaro M, Monconduit L, Buzsáki G (2005) Spike phase precession persists after transient intrahippocampal perturbation. Nat Neurosci 8:67–71